Laser Imprint Reduction Using a Low-Density Foam Buffer as a Thermal Smoothing Layer at 351-nm Wavelength

R. G. Watt, J. Duke, C. J. Fontes, P. L. Gobby, R. V. Hollis, R. A. Kopp, R. J. Mason, and D. C. Wilson
Los Alamos National Laboratory, Los Alamos, New Mexico 87545

C. P. Verdon
Lawrence Livermore National Laboratory, Livermore, California 94551

T. R. Boehly, J. P. Knauer, D. D. Meyerhofer, V. Smalyuk, and R. P. J. Town
Laboratory for Laser Energetics, University of Rochester, Rochester, New York 14627

A. Iwase and O. Willi
Imperial College of Science, Technology and Medicine, London, United Kingdom
(Received 8 June 1998)

Laser-nonuniformity-induced perturbation growth has been measured on planar foam-buffered plastic (CH) targets irradiated with 351-nm laser radiation. The maximum observed perturbation growth was reduced by about 50% by the foam buffer. Rayleigh-Taylor unstable growth of intentional mass modulations was minimally changed by the addition of the foam buffer. We conclude that the reduction of *laser-induced* perturbation growth is a result of a reduction in the perturbation seed amplitude rather than any changes in the growth rate in the solid due to preheating by radiation or shocks caused by the presence of the foam buffer. [S0031-9007(98)07706-0]

PACS numbers: 52.58.Ns, 52.35.Py, 52.40.Nk, 52.50.Jm

Target perturbations created by laser nonuniformity are a serious concern for direct drive inertial confinement fusion (ICF) implosions. Direct drive targets for the National Ignition Facility (NIF) [1] are expected to be particularly sensitive to perturbations with wavelengths of 100–500 μm (mode numbers 100–20). Perturbations in the wavelength range from 2 to 200 μm are produced by the speckle pattern associated with distributed phase plates (DPP). Combined with smoothing by spectral dispersion (SSD), DPP/SSD [2] will only average the speckle perturbation after several coherence times, leaving a residual imprint. This imprint can seed Rayleigh-Taylor (RT) instability in the shell of an imploding capsule, resulting in shell breakup and disruption of the implosion. Reduction of this seed or its subsequent growth is important to the ultimate success of direct drive ICF. One NIF direct drive target design controls growth by adding x-ray preheat using small amounts of a high-Z dopant in the ablator to raise the implosion isentrope. Alternatively, thermal smoothing in a preformed plasma may reduce the initial seed amplitude. This plasma can be formed either by a soft x-ray pulse incident on the solid shell prior to the laser drive [3] or by ionizing a low density foam buffer with the laser. Foam-buffered thermal smoothing has been studied both experimentally [4–7] and computationally [8–10]. It was noted experimentally [4] and computationally [9,10] that a thin high-Z layer coated onto the foam facing the laser side is important to preheat and ionize the foam supersonically. While tests with 527-nm lasers incident on foam targets have shown encouraging reductions in perturbation growth, data at the desired 351-nm wavelength has been needed.

This Letter presents the first 351-nm experimental results of *laser-induced*, foam-buffered instability growth, and of *mass-modulated*, foam-buffered RT growth. The *mass-modulated* RT measurements indicate that the presence of the foam buffer causes little change to the growth of imposed surface perturbations. We conclude that the reduction in observed *laser-induced* perturbation growth on flat targets in the presence of a foam buffer is due to foam imprint mitigation rather than preheat. Good agreement between the experimental data and hydrodynamic simulations has been obtained.

The experiment was conducted at the Omega [11] laser facility at the University of Rochester. Five drive beams having both DPP/SSD smoothing and distributed polarization rotators [12] were used to irradiate planar targets with and without mass modulations. A 2D-SSD IR bandwidth of 0.12×0.17 nm (0.25 THz) was used for RT growth measurements of imposed mass perturbations. The SSD modulator was turned off to study late time instability growth seeded by laser nonuniformity. The laser provided a nominal 3 ns flattop pulse with a 125 ps 10%–90% rise time containing approximately 1700 J total in the five drive beams. $f/6$ focusing optics were used. Uniform irradiance of 2×10^{14} W/cm^2 was obtained over a 650 μm diameter region of the target. A uranium backlighter target, separated from the main target by 9 mm, was illuminated by ten additional beams. The main target was imaged by a multiple pinhole, gated framing camera [13] with a time separation of 125 ps

 0031-9007/98/81(21)/4644(4)$15.00

between 80 ps exposures. A debris/preheat shield was placed between the main target and the backlighter. The Al and Be filters restricted the dominant backlighter radiation to the 1.1–1.5 keV region. The framing camera spatial resolution was 9–10 μm using 8 μm pinholes at a magnification of approximately 14.5. The framing camera/film system was characterized by using shots where the normal growth foil was replaced by a static knife edge, an Au grid, or transmissive CH foils with multiple thickness steps across the foil to check the modulation transfer function (MTF) and linearity of the camera system. The experimental configuration is similar to that used by Glendinning [14] for RT growth experiments on NOVA.

The targets were either smooth CH foils or CH foils with single mode sinusoidal modulations. The behavior of both types of targets was observed with and without a foam buffer on the side irradiated by the laser. The mass modulations were located on the ablation side of the target. The peak to valley (PV) modulation amplitude was usually 1 μm, with modulation wavelengths of 20, 31, or 60 μm. All solid substrates had a density of 1.05 g/cm^3 and a thickness in the range of 19–24 μm. The foam used in this experiment was 30 mg/cm^3 polystyrene, machined into a flat 100 μm thick plug with a surface finish of about 2.5 μm rms. The uniformity was dominated by the cell size of the foam (6 ± 2 μm diameter) rather than by any machining artifacts. The laser side of the foam was overcoated with a 15-nm (nominal) Au layer that acted as an x-ray flash source to ionize the foam supersonically.

Foil acceleration was studied using edge-on streaked x-ray imaging shots. The spatial and temporal resolutions were 25 μm and 10 ps, respectively. The measured rear-surface trajectory showed excellent agreement with 1D hydrodynamic code simulations for both bare and foam-buffered shots, using the measured power history. The hydrodynamic behavior was similar except for an additional 500 ps shock transit time across the foam. Figure 1 compares data to a LILAC [15] simulation of a foam-buffered CH foil.

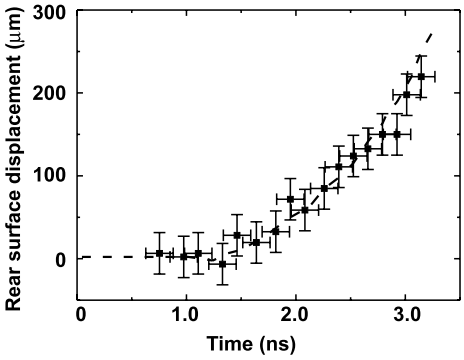

FIG. 1. Acceleration history for a foam-buffered CH foil compared to a 1D LILAC simulation.

Bare and foam-buffered *mass-modulated* targets were illuminated to characterize changes in the growth history due to the presence of the foam. Face-on framing camera images were taken up to 3 ns. Growth of the fundamental mode is shown in Fig. 2 for three different mass modulation wavelengths. The amplitude of the optical depth modulation (δOD) as a function of time is shown, after correction for the MTF of the camera system. The final amplitude of the modulation with a foam buffer present is comparable to that of a bare target. The optical depth modulation history is similar with and without the foam layer, except for the foam transit time delay. Only shots for which the laser power is the same to within 15% at all times were used in each plot. Despite similar shapes, in all cases it appears that the growth of the foam-buffered target starts from a lower level than the bare target. This reduction may be connected to the nonconformal interface between the foam and the sinusoidal modulations. If the foam growth data were shifted upward on any plot by the difference between the starting amplitudes observed, the time delay between the bare and foam-buffered growth would be approximately 500 ps, similar to the predicted and measured shock transit time in the 100 μm foam layer.

Mason *et al.* [10] showed calculationally that the principal cause for imprint reduction with a foam buffer is the high thermal conductivity of the buffer which acts to smooth the disturbances crossing it so that a nearly flat shock ultimately impinges on the CH foil. Simulations of the Omega shots with 1D NLTE LASNEX [16] have shown similar electron temperature profiles for the foam-buffered and bare foils. The electron temperature is $\approx$9 eV behind the shock, $\approx$80 eV at the ablation surface,

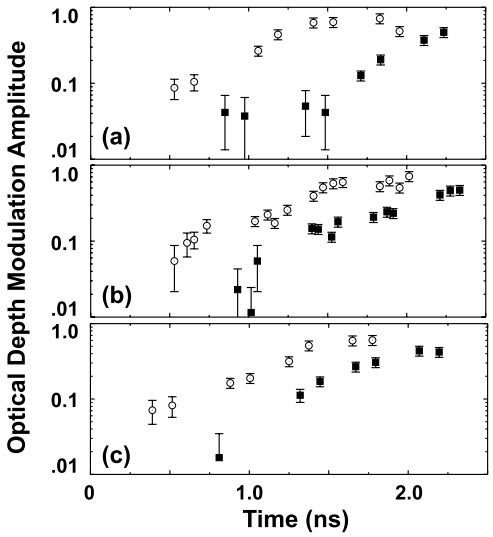

FIG. 2. Measured optical depth perturbation amplitudes for 20 μm (a), 31 μm (b), and 60 μm (c) growth, after correction for the MTF. The open circles are the bare data, and the solid squares are the foam-buffered data in each plot.

and ≈150 eV at the critical surface. Additionally, any change due to shock reflection off the foam/solid interface is minimal. LASNEX shows a 20% higher postshock density in the foil with the foam buffer (from shock overtaking) than without it. The foil adiabat is therefore similar for both targets. In the case of the foam buffer, both the increased Atwood number, due to the somewhat higher postshock density, and the lack of ablative stabilization at the foam/solid interface are destabilizing, which should result in increased growth which is not seen experimentally. All of this supports the picture of smoothing due to thermal conductivity in [10].

We compared the 60 μm wavelength growth data to 2D Eulerian simulations using POLLUX [17] (Fig. 3), because the smallest instrumental correction and error bars in *laser-induced* perturbation growth occur there. The simulations included the experimental power history but did not include the foam cell structure, the nonconformal foam/solid interface, or the speckle pattern of the laser. The solid curves in Fig. 3 are calculations done for nonpreheated foils and are in good agreement with the data. Note, however, that the foam calculation required a reduced initial amplitude (0.4 μm PV), reflecting the apparent reduced initial amplitude seen in the data. For reference, note that the lowest measured 60 μm bare growth data (δOD = 0.029) corresponds to 1 μm PV from the POLLUX calculations, while the peak measured modulation (δOD = 0.516) corresponds to 12 μm giving a growth factor of 12 in surface perturbation depth. Similar numbers apply to the foam-buffered 60 μm growth. The dashed curves show the effect of a preheat pulse on the foils equal to 10% of the peak laser irradiance, using a 100 eV Au radiation source, as a preheat sensitivity test. To account for the 50% reduction in *laser-induced* perturbation growth shown below, using preheat decompression rather than imprint mitigation, would require at least this 10% preheat level. (At 1.6 ns in Fig. 3, 10% preheat caused a reduction of 1.73 in the optical depth modulation in the foam simulation.) Such preheat appears inconsistent with the measured *mass-modulated* growth in Fig. 3, suggesting that preheat did not control the measured growth at this wavelength.

Experiments using smooth targets with SSD turned off to retain the DPP speckle pattern in the drive were carried out to evaluate foam imprint mitigation. The response of a bare target to this *laser-induced* perturbation at 2.2 ns is shown in Fig. 4, along with that of a foam-buffered target at 2.95 ns. The images, shown in optical depth space, have been corrected for the film response. The perturbation level in the foam-buffered case is significantly lower than the level in the bare target. Figure 5 shows the Fourier power spectra of a bare target at 2.45 ns (created by averaging the spectra at 2.2 and 2.7 ns) and the foam-buffered target at 2.95 ns. The data has had the instrument noise removed from it, and has been corrected for the instrument MTF [18]. The use of a composite bare power spectrum at 2.45 ns compensates for the nominal 500 ps shock transit time in the foam. The data for foam at frequencies larger than 45 mm^{-1} is at the instrument noise floor. The reduction in amplitude at 60 μm wavelength (16.7 mm^{-1}) is almost a factor of 2.0. As discussed above, sufficient preheat to produce this level of reduction would result in growth inconsistent with that seen in the case of the *mass-modulated* 60 μm growth in Fig. 3.

Although the present experiment used a 3 ns flattop drive at 2×10^{14} W/cm^2, foam buffering can also be applied to a shaped pulse direct drive NIF target, without major effects on the implosion. Replacing 10 μm of the deuterium-tritium (DT) fuel on the outside of Verdon's [19] target with 50 μm of CH foam at 50 mg/cm^3 plus a 25-nm Au overcoat produces a foam-buffered fuel adiabat very similar to that of the original bare target. An additional 1% energy increment was needed, increasing the power in the first three pickets in Verdon's drive pulse by a factor of 1.5–2. Radiative preheat increases the temperature in the DT fuel ahead of the first shock, but it remains below 0.3 eV (as compared to 3 eV in the solid for this experiment). Foam smoothing of nonuniformities at 2×10^{13} W/cm^2 during the first pulse remains an issue, but we have successfully shown mitigation in foam

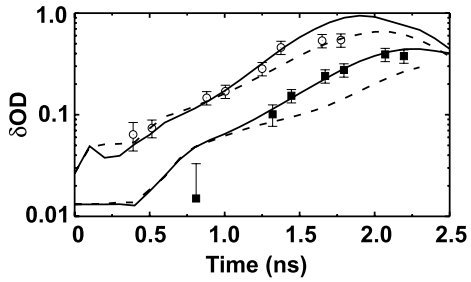

FIG. 3. Comparison between measured 60 μm growth data for bare (open circles) and foam-buffered (solid squares) growth and 2D simulations. The calculations include the camera MTF correction. The solid curves are for nonpreheated foils. The dashed curves contain an additional preheat pulse equal to 10% of the incident laser irradiance, from a 100 eV Au x-ray source.

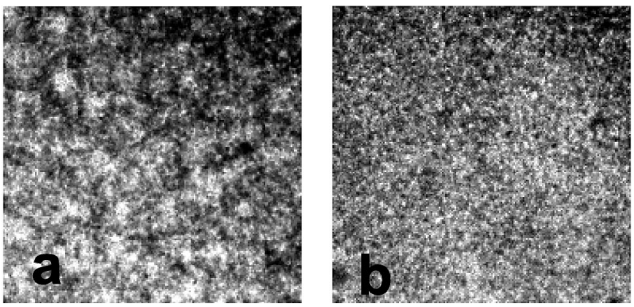

FIG. 4. Face-on radiographs of laser-nonuniformity-induced growth at 2.2 ns on a bare plastic foil (a) and at 2.9 ns on a foam-buffered target (b).

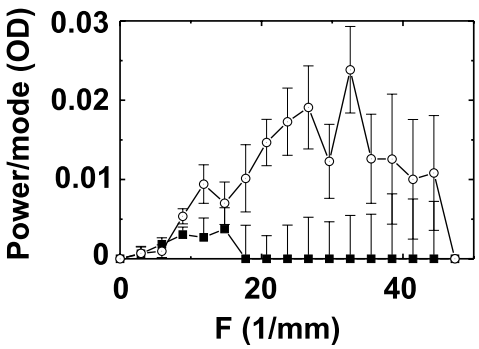

FIG. 5. Optical depth power spectra for a bare target (open circles) at 2.45 ns and a foam-buffered target (solid squares) at 2.95 ns. The instrument resolution limit is greater than 50 mm^{-1}. The spectra converge below 5 mm^{-1} due to the finite size of the sample.

buffer experiments at 527 nm at intensities as low as 1×10^{13} W/cm^2, suggesting that 351-nm operation at these low intensities may be possible.

In summary, detailed measurements of RT growth from thin planar foil targets with sinusoidal mass modulations have demonstrated that foam coatings do not significantly change the growth of those modulations. This implies that the observed reduction in *laser-induced* perturbation growth in the presence of the foam is the result of imprint mitigation rather than changes in the sensitivity of the target to perturbations. Smooth targets driven by non-SSD beams exhibit pronounced perturbations that may be suppressed by a foam buffer between the laser and the solid surface by factors of 1.75–2 in the wavelength range from 40 to 200 μm. The data demonstrate that the primary benefit of a foam buffer is the thermal smoothing of laser nonuniformities that ultimately reach the solid target. The degree of smoothing caused by the foam buffer relative to the bare target marginally exceeds the smoothing found with 0.25 THz 2D SSD on other bare targets, in the case of the square laser pulse used in this experiment. The use of a foam buffer combined with full beam smoothing would be expected to produce an even better imprint reduction, but would have been beyond the ability of the present experiment to resolve. The application of foam to a NIF target design has been shown. If the foam buffer can be shown to work at low intensity in the blue, it may have significant impacts on *laser-induced* perturbation growth in direct drive NIF implosions.

The authors thank the Omega operations crew whose hard work and dedication allowed the successful execution of these experiments. Target assembly was done at Omega, and production and machining of the foam was done in the target fabrication group at Los Alamos National Laboratory. This work was performed under the auspices of the U.S. Department of Energy, DOE Contract No. W-7405-ENG-36.

[1] S. W. Haan *et al.,* Phys. Plasmas **2**, 2480 (1995).
[2] S. Skupsky *et al.,* J. Appl. Phys. **66**, 3456 (1989).
[3] M. Desselberger *et. al.,* Phys. Rev. Lett. **68**, 1539 (1992).
[4] M. Dunne *et al.,* Phys. Rev. Lett. **75**, 3858 (1995).
[5] T. Afshar-rad *et al.,* Phys. Rev. Lett. **73**, 74 (1994).
[6] R. G. Watt *et al.,* Phys. Plasmas **4**, 1379 (1997).
[7] D. Hoarty *et al.,* Phys. Rev. Lett. **78**, 3322 (1997).
[8] M. H. Emery *et al.,* Phys. Fluids B **3**, 2640 (1991).
[9] M. Desselberger *et al.,* Phys. Rev. Lett. **74**, 2961 (1995).
[10] R. J. Mason *et al.,* Phys. Plasmas **5**, 211 (1998).
[11] T. R. Boehly *et al.,* Opt. Commun. **133**, 495 (1997).
[12] T. R. Boehly *et al.,* in *Laser Interaction and Related Plasma Phenomena,* edited by G. H. Miley and E. M. Campbell, AIP Conf. Proc. No. 406 (AIP, New York, 1997).
[13] P. Bell *et al.,* Proc. SPIE **1801**, 1140 (1992).
[14] S. G. Glendinning *et al.,* Phys. Rev. Lett. **80**, 1902 (1998).
[15] An earlier version of LILAC is described in Laboratory for Laser Energetics, Report No. 16 (unpublished).
[16] G. B. Zimmerman and W. L. Kruer, Comments Plasma Phys. Controlled Fusion **2**, 51 (1975).
[17] G. J. Pert, J. Comput. Phys. **43**, 111 (1981).
[18] V. Smalyuk *et al.,* Rev. Sci. Instrum. (to be published).
[19] C. P. Verdon, Bull. Am. Phys. Soc. **38**, 2010 (1993).